8

Squeeze Casting of Al-Si Alloys

Bellisario Denise[1], Boschetto Alberto[2], Costanza Girolamo[1], Tata Maria Elisa[1], Quadrini Fabrizio[1] and Santo Loredana[1]
[1]*Department of Mechanical Engineering, University of Rome Tor Vergata,*
[2]*Department of Mechanics and Aeronautics, University of Rome La Sapienza, Rome,*
Italy

1. Introduction

Nowadays there is a great demand of lightweight parts with high mechanical performances; in such applications, e.g. automotive, production rate and process control are critical aspects as well. This way, pressure assisted casting processes are a good compromise between performances and costs. Over the past decade, aluminium or magnesium components produced by means of pressure assisted processes have been introduced to substitute cast iron components. When the substitution is possible, a great advantage in terms of cost saving and component weight reduction is obtained.

The main technological issue in the development of new pressure assisted casting processes is related to the increase of the holding pressure during the alloy solidification. In fact, it is evident that, by increasing the pressure, the overall quality of the casting generally increases in terms of a smoother surface, lower porosity and higher mechanical properties. In die casting, higher holding pressures lead to higher production runs too. However, it is not yet clear what is the main role of the pressure during casting as many other process parameters are present and their effect cannot be easily separated from the effect of the pressure. Moreover, different results may be obtained depending on the alloy to cast and on its sensibility to the casting process. In this study, several experiences were collected which show the effect of the pressure during the squeeze casting of Al-Si alloys. The squeezing systems were designed on purpose to point out different aspects of the squeezing process: the effect of the pressure at constant cooling rate, the mechanical property distribution in the casting, the expected properties for the Al-Si alloy. Numerical modelling of the squeezing operations allowed to evaluate the limits of the production systems and to provide general conclusions. The combination of the proposed squeezing systems and the related numerical models is the main result of the current work as well as the prediction of the Al-Si alloy mechanical properties as a function of the squeezing pressure.

For aluminium alloys, the application of a holding pressure during cooling plays a very important role in defining casting properties. A significant microstructural refinement was already observed during the solidification of an Al-Cu alloy under high pressure (Han et al., 1994). In this case the average dendrite cell size changes from 30 μm, without applied

pressure, to 5 μm under 1.7 GPa. For an Al-Si alloy (designated as B390) a great microstructure refinement was also observed as a consequence of the pressure application (up to 100 MPa) and higher mechanical properties were measured in terms of hardness and tensile strength (Maen et al., 2000; Lee et al., 2000) but no material model has never been proposed. Other studies showed that in direct and indirect squeeze casting, apart from the pressure, other process parameters strongly affects microstructure and mechanical properties such as melt and die temperature (Maen et al., 2000; Lee et al., 2000), die geometry (Kim et al., 1999) and melt flow (Lee et al., 2000). In such conditions, it is very difficult to understand what process parameter is the main one in determining the final mechanical properties of the cast alloy. As pressure increases, together with microstructure refinement, other structural modifications can occur such as shrinkage, porosity change (Hong et al., 1998a) and macrosegregation (Hong et al., 1998b; Gallerneault et al., 1995; Gallerneault et al., 1996). As a result, a complete process map can be obtained with the definition of the process window where no micro and macro-defects occur (Hong et al., 1998a; Hong et al., 1998b). Also for aluminium matrix composites, a positive effect of the applied pressure was observed for mechanical properties (Shuangjie and Renjie, 1999). However all these studies do not show a way to predict the final performances of the cast alloy depending on the casting conditions.

From a theoretical point of view, the effect of the pressure application can be divided into two contributions: a direct and an indirect one. The first one is related to the alloy phase diagram modification. Thermodynamic equilibrium curves shift toward higher temperatures as pressure increases. For aluminium alloys (and generally for metals) the transformation temperature shift is expected to be negligible as the phase diagram of the alloy minimally changes with the pressure (Savas et al., 1997). A second direct effect is related to the porosity reduction. In fact at high pressures, entrapped gases remain in solution without cavity formation (Kalpakjian, 2000). Also shrinkage porosity formation is prevented. As a consequence, the resulting metal density is higher. A last direct effect is also macrosegregation (Hong et al., 1998a) even if a strong dependence on the cooling rate is also present. On the other hand the pressure indirect effect is related with the cooling rate. Allowing the better contact between the mould and the cast part during solidification, pressure enhances heat transfer, increasing cooling rate. As a consequence, a lower grain size is observed inside the component also far from the external surface. Actually, pressure is not the only parameter which influences the cooling rate (the melt and die temperature, the melt flow condition and the process times are important as well) but it's surely the most easily adjustable.

At present, it's not clear if direct and indirect pressure effects have the same importance in defining the cast mechanical properties. This way, it's not possible to establish if a pressure increase could be a convenient practice when porosity is not a problem and significant changes of the cooling rate are not expected. It is not a secondary problem as a pressure increase leads to a cost increase. On the other hand, the cooling rate evaluation is generally a very difficult task for all the casting processes and in particular for aluminium alloy squeeze casting. In fact, cooling rates can reach very high values and a direct temperature measurement is practically impossible due to the mould thermal inertia. Cooling rate is never directly measured except for some cases when thermocouples are inserted inside the

casting. Lee et al. studied the effect of the gap distance on the cooling behaviour and the microstructure of an indirect squeeze cast and gravity die cast aluminium alloy. They inserted thermocouples through the die, located at the centre of each casting. However a numerical model was used to calculate the temperature profile and was preferred for the cooling rate extraction due to the intrinsic dispersion of the measured cooling curves (Lee et al., 2002). In fact, too many factors affect the temperature profile during casting, from melt turbulence during injection to mould transient phase. Britnell and Neailey placed thermocouples inside the die near the mould-melt interface to study the macrosegregation in thin walled squeeze cast samples but thermal traces can be used just for a qualitative analysis (Britnell et al., 2003).

In order to study squeeze casting, it is very important to evaluate the influence of the pressure direct and indirect effects. For this purpose, in the current study, two sets of Al alloy samples were fabricated: the first set by using different applied pressures and same cooling rate; the second one by using the same applied pressure but different cooling rates. Moreover, a finite element (FE) model was set up so as to simulate the thermal history inside the mould during the heating-cooling sequence. A maximum cooling rate was estimated in this case, resulting from the chosen mould geometry.

Another important aspect under investigation is the material behaviour simulation and the prediction of mechanical property distribution in large ingots. A different squeezing system was designed for this purpose and other two sets of samples were produced. A suitable FE model was also defined which permits to gather the properties of an aluminium part when its geometry and process history are known. In a reverse approach, as local mechanical testing can be always performed on cast parts, the cooling rate could be inferred from the mechanical properties resulting from the tests. This information can be used for process optimization as well as for the validation of process numerical simulations.

2. Material modelling

A simple law which correlates mechanical properties (yield strength and Vickers hardness) with cooling can be extracted from the scientific literature. First, the average grain size can be correlated to the mechanical properties by Hall-Petch (Reed Hill, 1996):

$$\sigma_Y = \sigma_0 + K_Y \lambda^{-1/2} \tag{1}$$

$$HV = HV_0 + K_H \lambda^{-1/2} \tag{2}$$

This equation was also proposed for the prediction of mechanical properties of reinforced aluminium specimens (Shuangjie and Renjie, 1999). Furthermore, a simple relationship between the cooling rate (ε) and the average dendrite cell size (λ) was used for aluminium alloys too (Han et al., 1994; Kim et al., 1999):

$$\lambda = B\varepsilon^n \tag{3}$$

Combining equations (1), (2) and (3), a direct correlation between the cooling rate and both the final yield strength and the hardness is obtained:

$$\sigma_Y = \sigma_0 + C_Y \varepsilon^m \text{ where } \begin{cases} C_Y = K_Y B^{-1/2} \\ m = -\dfrac{n}{2} \end{cases} \quad (4)$$

$$HV = HV_0 + C_H \varepsilon^m \text{ where } C_H = K_H B^{-1/2} \quad (5)$$

If the pressure indirect effect is predominant on the direct one, equations (4)-(5) can be used in order to predict the alloy mechanical properties with pressure during solidification.

3. Aluminium alloy

The examined material, aluminium alloy EN-AB46000, has nominal composition (wt.%) showed in the following Table 1. EN-AB46000 is a hypoeutectic Al–Si alloy, normally used in die casting processes. This alloy is universally known for its good castability, except for a little tendency towards forming surface and internal cavities caused by shrinkage during solidification.

Si	Fe	Cu	Mn	Mg	Cr	Ni	Zn	Pb	Sn	Ti	Al
8.0–11.0	0.6–1.1	2.0–4.0	0.55	0.15–0.55	0.15	0.55	1.20	0.35	0.25	0.20	To balance

Table 1. Al alloy composition (EN-AB46000).

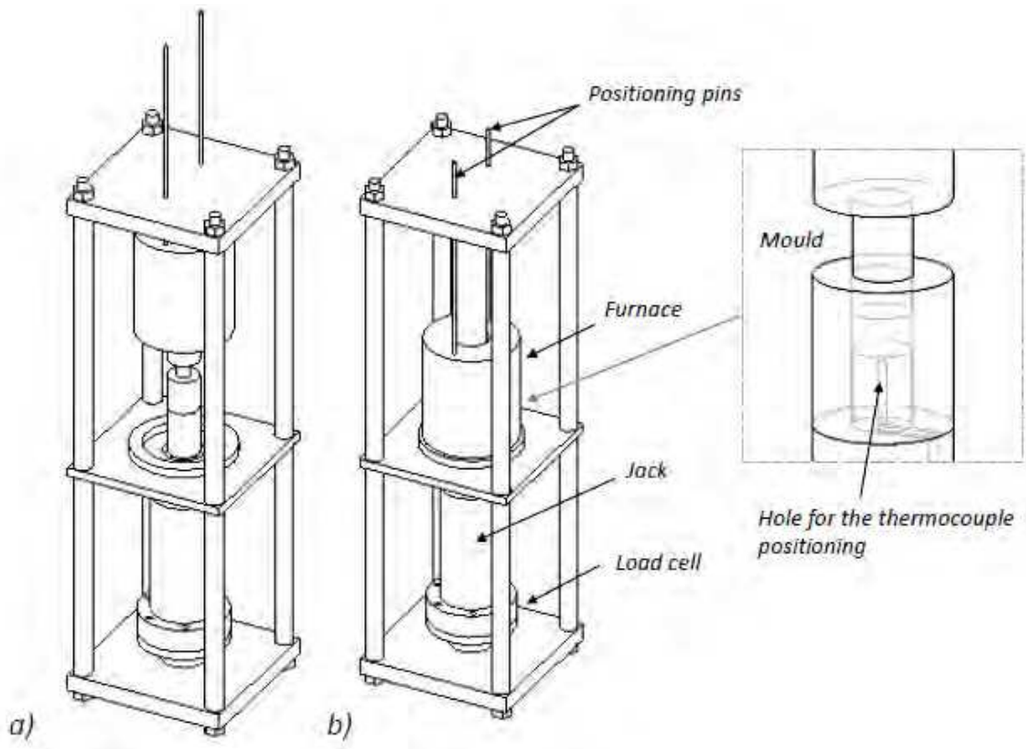

Fig. 1. 3D- sketch of the experimental apparatus: (a) Furnace position during the solidification; (b) Furnace position during the melting.

4. Study of the effect of the squeezing pressure

4.1 A squeezing system for small samples

In order to underline the effects of the pressure in squeeze casting, an original experimental apparatus was built. This kind of apparatus was made to cast samples under different pressure and cooling rate conditions. The experimental system was designed to melt the aluminium alloys directly in the mould and to apply the established pressure before starting the sample solidification. An on line acquisition system was defined for temperature and pressure data. The apparatus (Figure 1) consisted essentially in a frame, a mould, a resistance furnace, a thermocouple, a load cell and a jack. The cylindrical-shaped mould was enclosed by the coaxial resistance furnace (power 700 W). The furnace could be moved after the sample melting. The piezoelectric load cell, located near the furnace below the jack, had the maximum load of 1000 kg. Considering that the mould cavity had a 15 mm diameter, the maximum achievable pressure was about 56 MPa. The thermocouple was placed inside the mould in a hole made at the bottom. The AISI 303 steel was chosen to fabricate the frame and the mould.

During experimentation, the aluminium alloy was melted inside the mould and subsequently it was squeezed until its solidification. Two different process conditions were used. For the first condition, several pressures were applied, leaving the cooling rate approximately constant. In the second condition, the pressure was kept constant whereas the cooling rate was changed. The same initial melt temperature was considered in both cases. Due to the high thermal capacity of the steel mould in comparison with the aluminium alloy sample, the sample cooling rate depended only on the heat transfer between the mould and the air and no effect of the applied pressure was observed.

First fabrication condition					
Applied load [N]	*Applied pressure [MPa]*	*Initial melt temperature [°C]*	*Melt temperature at the pressure application [°C]*	*Mould cooling condition*	*Cooling rate [°C/s]*
0	0	640	600	In air	0.7
2500-6500	14-37	640	600	In air	0.9
Second fabrication condition					
Applied load [N]	*Applied pressure [MPa]*	*Initial melt temperature [°C]*	*Melt temperature at the pressure application [°C]*	*Mould cooling condition*	*Cooling rate [°C/s]*
6500	37	640	600	Water spray	1.9
6500	37	640	600	Compressed air flow	5.9
6500	37	640	600	Compressed air with aqueous suspension flow	10.45

Table 2. Process parameters for aluminium alloy sample fabrication.

Table 2 summaries the process variables used for the specimen fabrication. All the samples had cylindrical shape with a diameter of 15 mm and a height of 3 mm. Each specimen was

preliminarily subjected to mechanical polishing and subsequently etched with 1% aqueous HF so as to reveal its microstructure. Observations were made with an optical microscope. FIMEC (Flat-top Cylinder Indenter for Mechanical Characterization) and Vickers microhardness tests were performed on the samples.

The FIMEC test (Donato et al., 1998) is based on the penetration, at constant rate, of a flat punch of small size (a diameter of 2 mm and a height of 1.5 mm). During the test, the applied load and the penetration depth are measured, therefore load vs. penetration (LP) diagrams can be recorded. The characteristics of LP curves were described in detail in previous works (Gondi et al., 1996): the limit load q_Y is reached after an initial linear stage, which is followed by a work-hardening-like stage with loads tending to a saturation value q_S. Indeed material work hardening starts much before the q_Y load during indentation. In such standardized conditions (penetration rate ≅ 0.1 mm/min and deformation rate in tensile test ≅ 10^{-3} s^{-1}), $q_Y/A \cong 3\ \sigma_Y$ and $q_S/A \cong 3\ \sigma_U$ where A is the area of the flat pin. A WC indenter of 2 mm in diameter, a 10 N pre-load, a 0.1 mm/min penetration rate and a 0.5-1 mm penetration depth were used for testing.

4.2 Experimental results

The microstructures of two solidified samples with different pressures (14 MPa and 37 MPa) at the cooling rate of 0.9 °C/s are showed in Figure 2. In both cases, the microstructures are similar and show primary aluminium dendrites, particles and eutectic constituents. In the same figure it is reported also the comparison between the resulting mechanical data. Also for other specimens, fabricated at different pressures but with the same cooling rate, comparable microstructure and mechanical data were obtained.

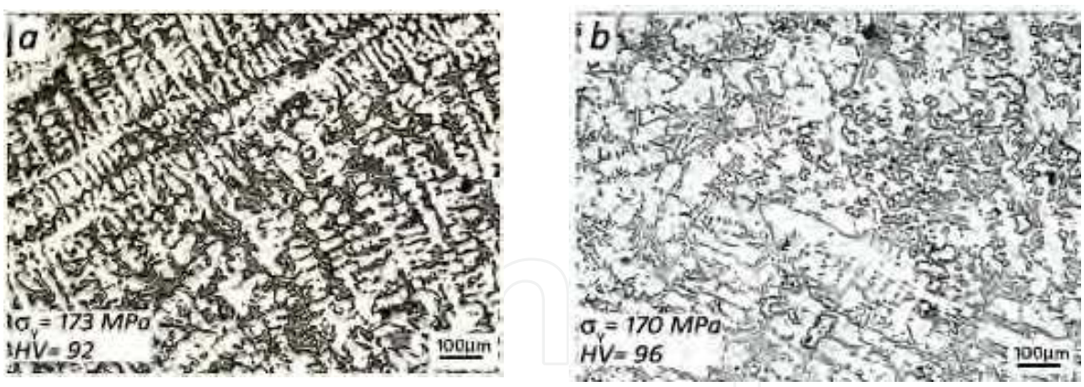

Fig. 2. Micrographs of metallographic sections and mechanical data of samples solidified at the pressure of 14 MPa (a) and 37 MPa (b) and the cooling rate of 0.9 °C/s.

Table 3 shows mechanical and microstructural data extracted from specimens produced both with the first and the second set of process parameters. In Figures 3 and 4 the micrographs of the metallographic sections of the samples are reported as well. In particular, Figure 3 shows the micrographs of an as-received-cast ingot together with micrographs of solidified samples with the first set of process parameters. In Figure 4, micrographs of samples solidified with different cooling rates but the same pressure of 37 MPa are shown.

Experimental results show that the pressure direct effect is negligible compared to the indirect one, at least in the considered pressure range. In fact, Figure 2 shows that, with the same cooling rate, no significant modifications occur in microstructural characteristics and mechanical properties. On the other hand, Figures 3-4 and Table 3 indicate that the greater the cooling rate the higher the Vickers microhardness and yield strength values due to the finer microstructure. These results were obtained thanks to the experimental apparatus, able to obtain samples at different pressures with the same cooling rate and vice versa. Moreover, the sample size is sufficiently small so as to assume that, inside the sample, an uniform distribution of the final mechanical properties is present.

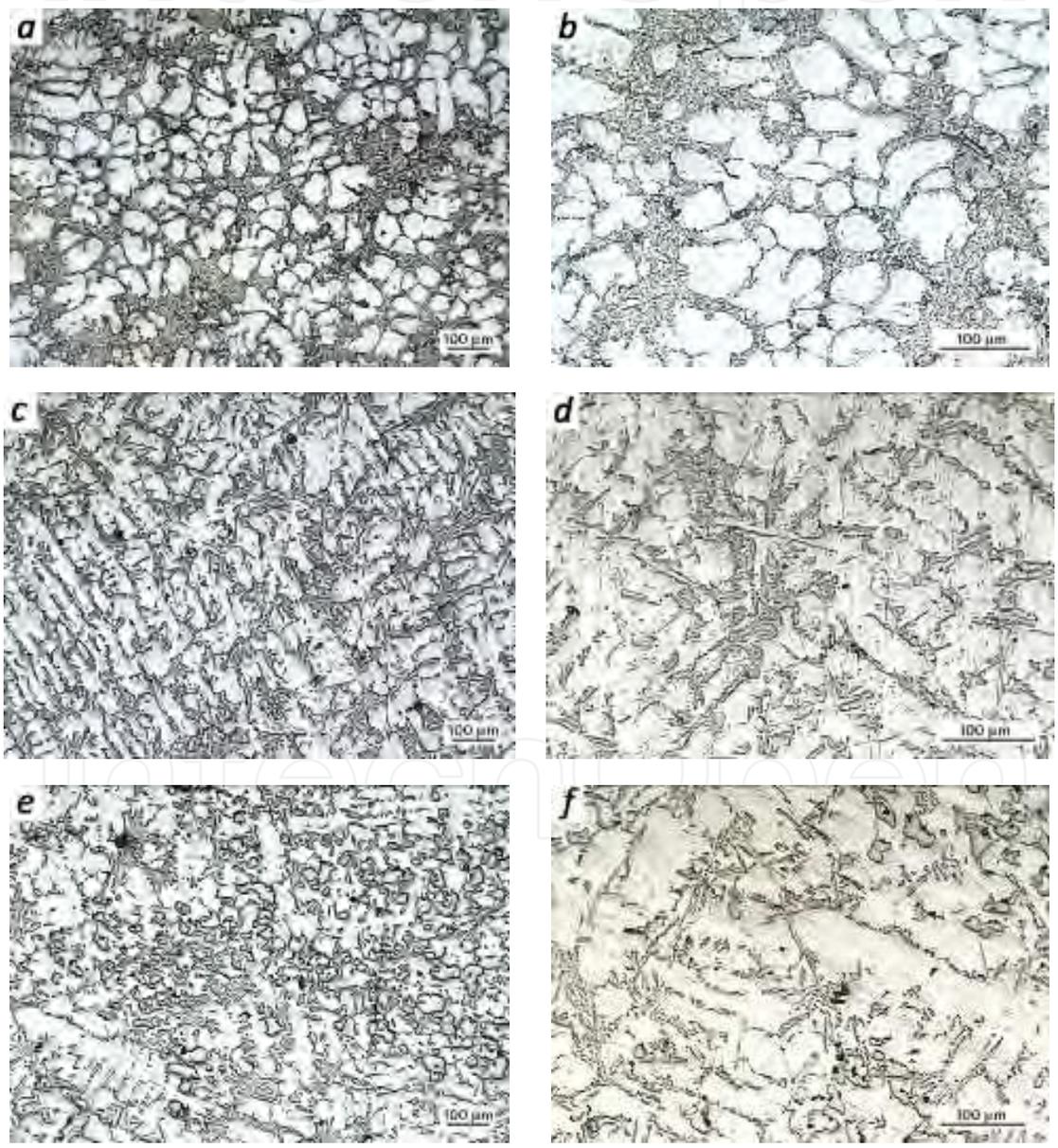

Fig. 3. Micrographs of metallographic sections of sample A (a,b), B (c,d) and C (e,f).

Some experimental thermal curves are reported in Figure 5, where the pressure effect on the cooling rate is separated from the mould cooling condition effect. The attention was focused in the cooling stage.

As a consequence of the pressure direct effect predominance, equations (4) and (5) can be used for the prediction of the material properties, considering the cooling rate as the only process parameter. Actually, the cooling rate is not directly adjustable, as it is function of the other process variables such as the melt and die temperature, the applied pressure and the cast geometry. Figures 6, 7 and 8 show that experimental data have a good fitting by means of the proposed equations (1-5). Particularly for equations (1)-(2) in Figure 6, presented data are also in good agreement with data extracted from literature (Han et al., 1994; Kim et al., 1999) for Al-Cu alloys. This occurrence suggests that the relationship between the cooling rate and the dendrite cell size could be expanded to the whole Al alloy family but further investigation would be necessary.

Some important considerations can be extracted from the experimental results so as to optimize a pressure assisted casting process. If the pressure direct effect remains negligible also for higher pressure values, there is no reason in increasing the pressure of a casting process. With the pressure level is sufficient to avoid porosity, it is advisable to use the minimum pressure value which leads to a high cooling rate. This way, it is also possible to change the other process parameters, such as the melt and die temperature, if that is a less expensive procedure. For example, in the squeeze casting process, similar mechanical properties can be obtained by reducing the pressure and decreasing contemporaneously the die temperature, if the preventive solidification can be avoided.

Samples	**Pressure [MPa]**	**Cooling rate [°C/s]**	**Average dendrite cell size [μm]**	**HV**	**σ_Y [MPa]**
A (as received)	0	-	48.9	81	150
B	0	0.7	37.1	92	147
C	37	0.9	36.6	94	160
D	37	1.9	33.1	95	173
E	37	5.9	20.3	117	199
F	37	10.5	16.6	116	200

Table 3. Mechanical and microstructural data extracted from the samples.

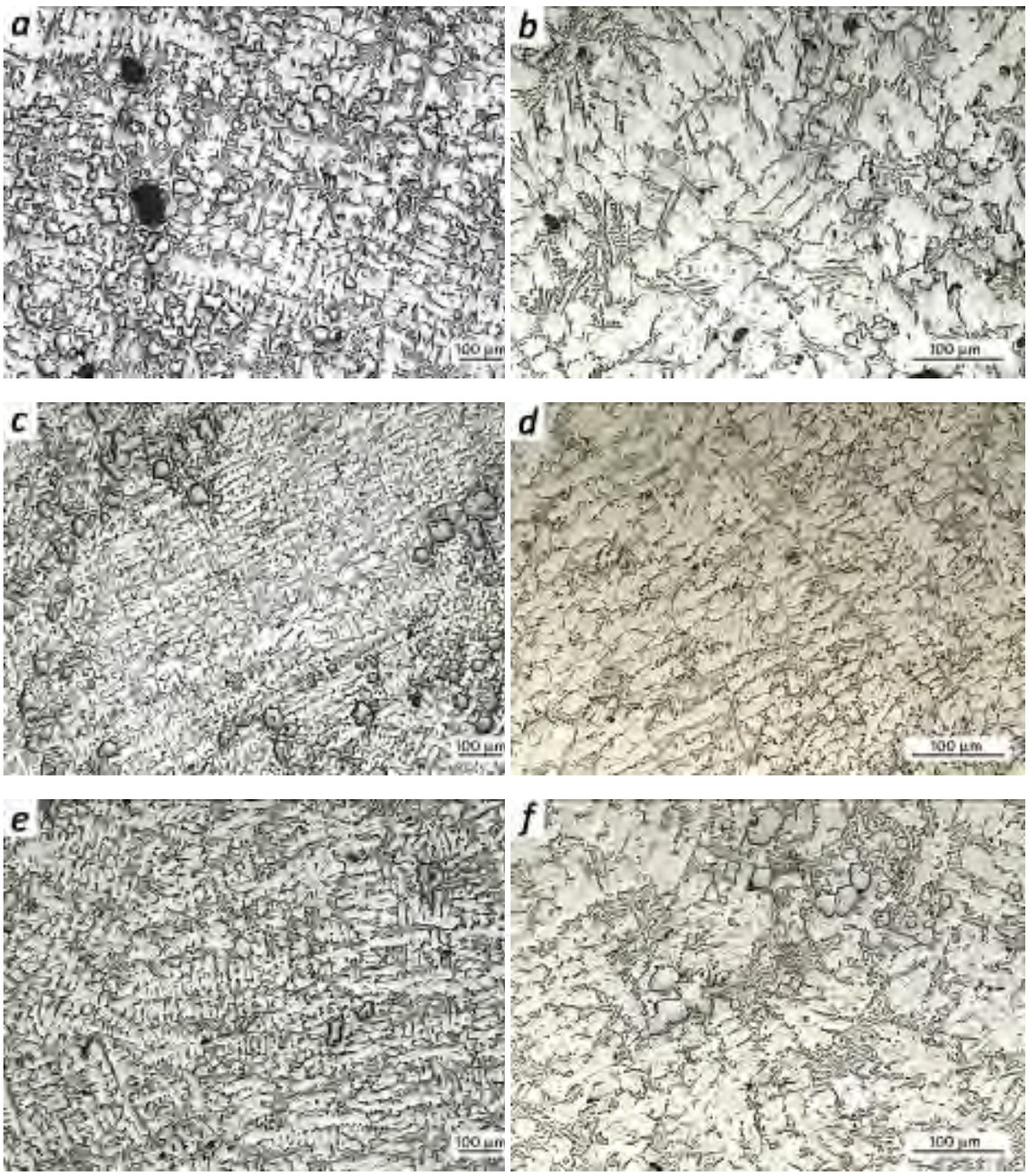

Fig. 4. Micrographs of metallographic sections of samples solidified with a pressure of 37 MPa and different cooling rates: D (a,b), E (c,d), F (e,f).

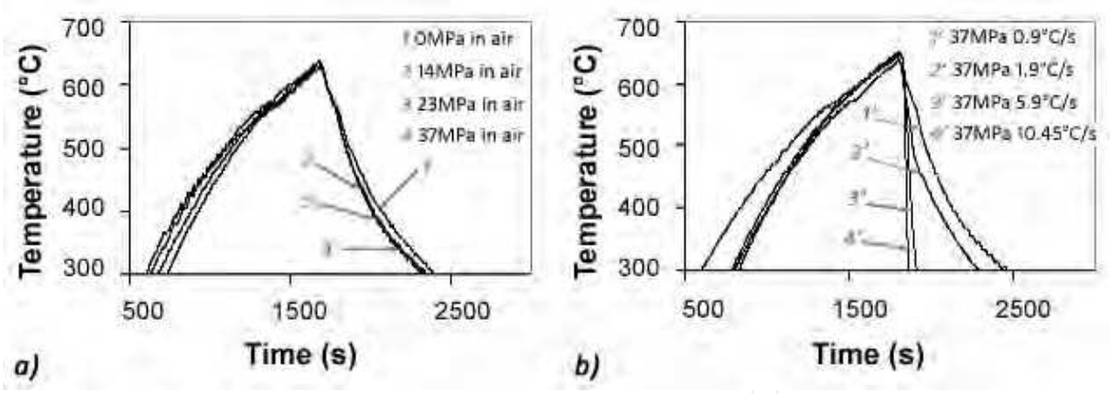

Fig. 5. Effect of pressure and cooling conditions on cooling rate.

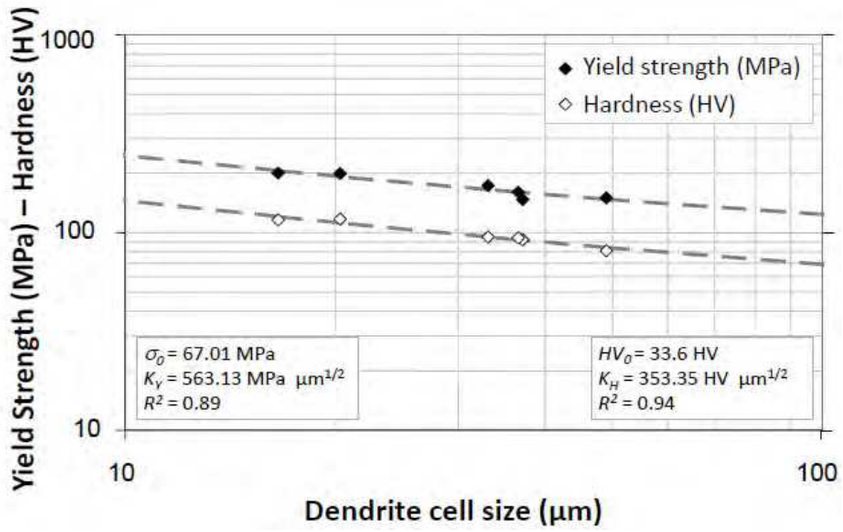

Fig. 6. Yield strength and Vickers hardness as a function of the dendrite cell size.

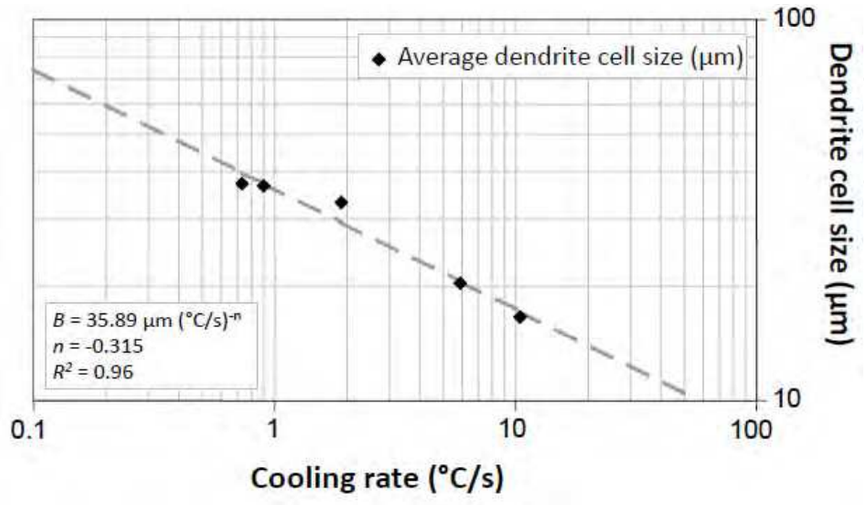

Fig. 7. Average dendrite cell size as a function of the cooling rate.

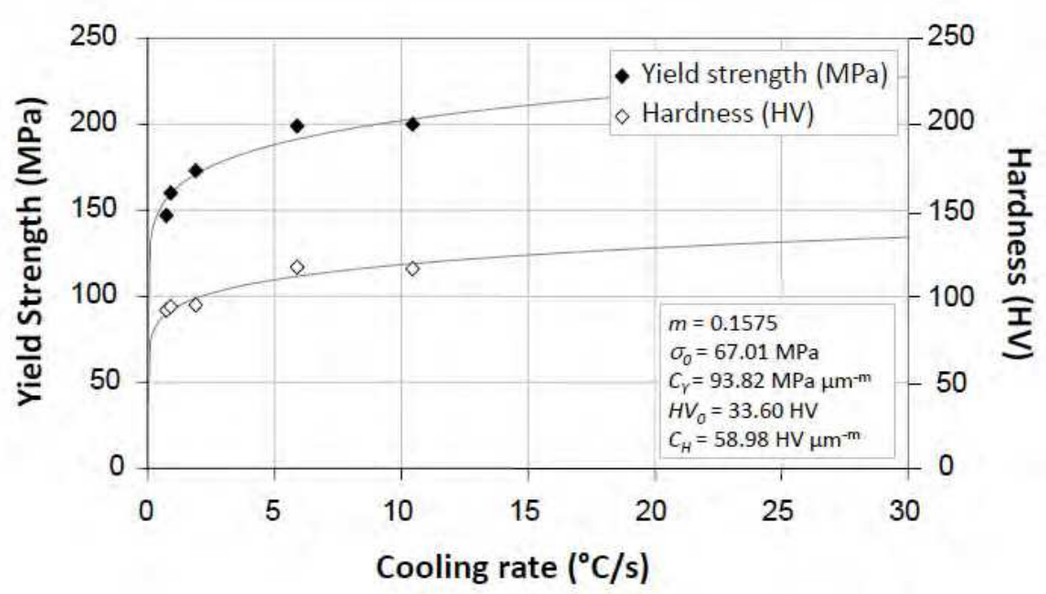

Fig. 8. Yield strength and Vickers hardness as a function of the cooling rate.

Equations (4)-(5) are particularly important, as they show the advantage that it is possible to reach by increasing the cooling rate. Evidently, it is not convenient to increase the cooling rate if the actual process is already positioned on the plateau of the curve of Figure 8. In this case, great changes of the cooling rate would produce small modifications of the mechanical properties. Equations (4)-(5) can be also used in a reverse way: measuring the properties of an aluminium alloy casting, it is possible to extract the cooling rate during its solidification. In particular, by using hardness measurements, a complete process control can be carried out if indentations are made on the overall geometry of the cast part. Dealing with the small size of the samples, the application of a miniaturized FIMEC test seems to be the only way for a proper material characterization.

4.3 Numerical simulation for the evaluation of the squeezing system performances

In order to simulate the heating-cooling sequence during the sample production, a FE axy-symmetric thermal model was built by discretising the mould geometry. The model is shown in Figure 9 where the material properties used are also reported. Generic values for an aluminium alloy and a stainless steel were used for these properties. Particularly for the aluminium alloy, a linear variation of the enthalpy was considered from the liquidus temperature to the solidus one. The applied thermal load depended on the convective heat transfer acting on the external surfaces.

Several analyses were performed by means of the described FE model. Initially the heating was modelled assuming that the convection bulk temperature T_b changes as a consequence of the furnace heating meanwhile the heat transfer coefficient h was constant and fixed arbitrarily at 50 W/(m^2 K), and the initial material temperature was 25 °C. The bulk temperature curve, as a function of time, was extracted fitting an experimental curve by means of the FE model. Being all the experimental curves identical during the heating, whatever curve could be used for this calibration. At the end the of the calibration

procedure, the obtained dependence of the bulk temperature versus time (Figure 10) substitutes, inside the model, the action of the furnace which is not directly modelled.

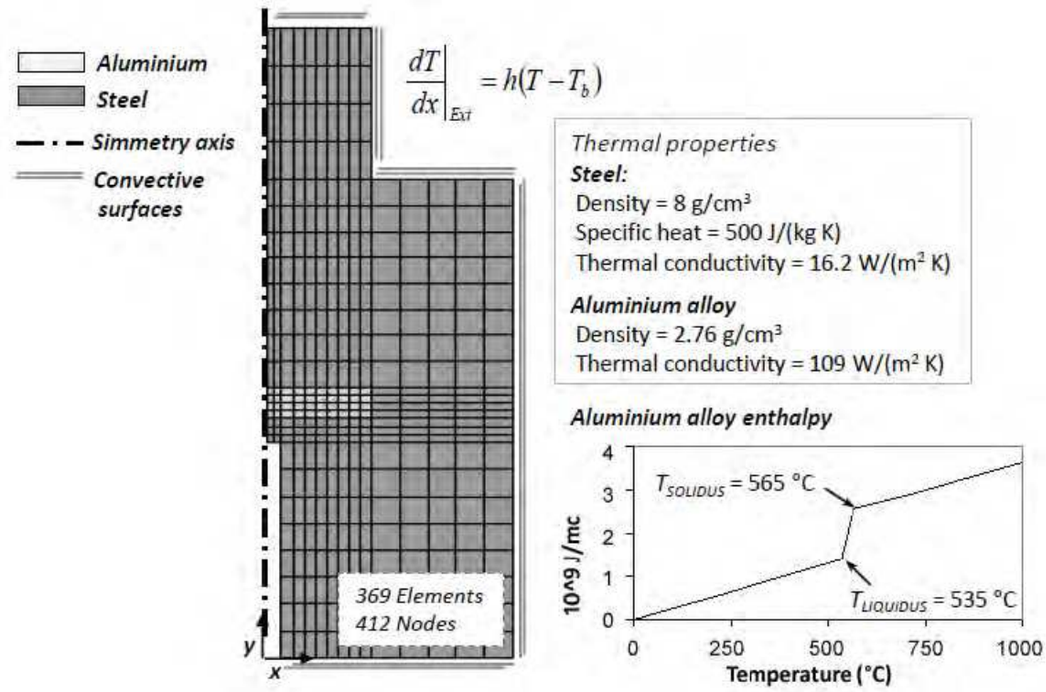

Fig. 9. The FE model.

After calibration, other thermal analyses were performed to simulate the cooling phase. In this case, at the end of the heating stage, a 25 °C constant value of the bulk temperature was applied to the convective surfaces, simulating the furnace removal. The different cooling conditions experimentally applied were simulated by changing the heat transfer coefficient *h*, which was always assumed constant along all the external surfaces. Figure 11 depicts the thermal map at the end of the heating phase. This map is approximately identical for all the fabrication conditions. In the same figure it is also reported the dependence of the cooling rate on the applied heat transfer coefficient. Furthermore, in the last graph, the experimental cooling rates are also reported.

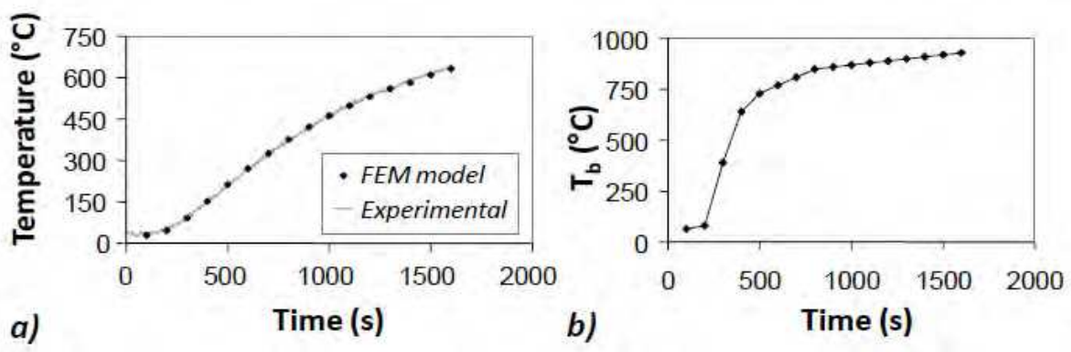

Fig. 10. FE model calibration.

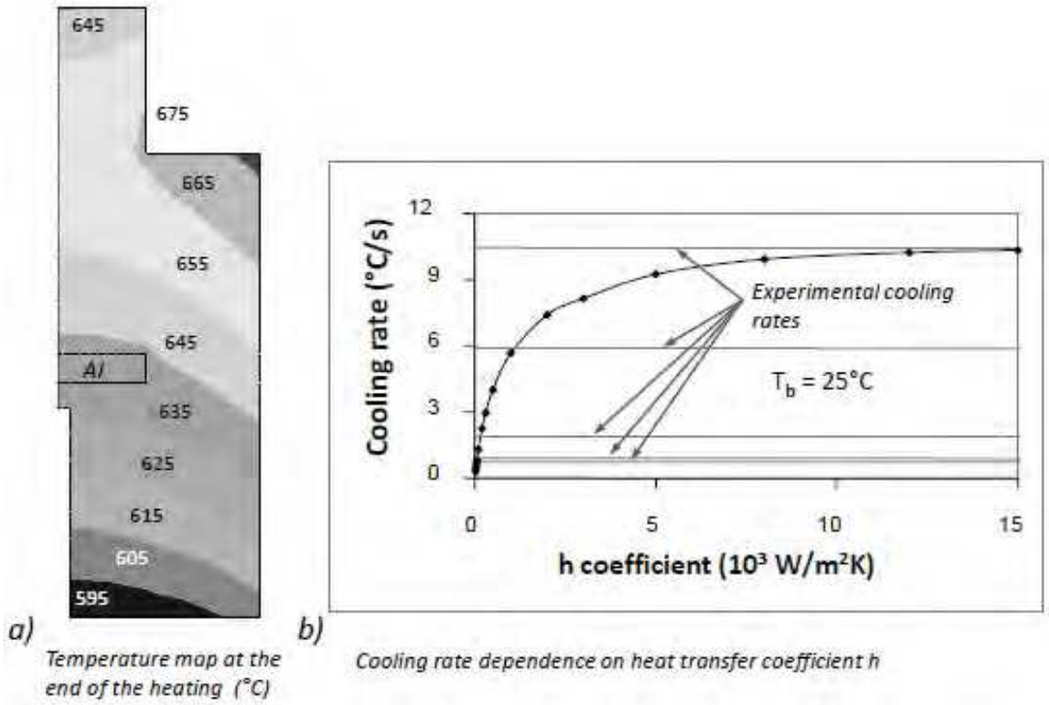

Fig. 11. FEM results: (a) Temperature map; (b) Cooling rate vs heat transfer coefficient.

Numerical results (Figure 11) show that a plateau in the cooling rate value is present if only the mould heat transfer condition changes. The higher experimental cooling rate is close to this numerically evaluated plateau, therefore no further significant decrease in the cooling rate can be expected by acting on the mould external walls. Actually, the proposed thermal model does not contain all the features to fully simulate the thermal problem. As an example, no thermal contact resistance was considered between the aluminium melt and the steel. This simplification is due to the fact that the temperature was experimentally acquired in only one point due to the limited size of the sample. In a more complex model, other calibrating constants would be present and more acquisition points would be necessary as well. Under these assumptions, all the neglected thermal aspects (such as the thermal resistance or the irradiation) are all taken into account globally by means of the same convective constants. However, FE modelling was important during experimentation, being possible to predict the limits of the experimental procedure and to understand the physical phenomena at the basis of the experiences.

5. Mechanical property distribution

5.1 A new squeezing system for larger ingots

In the first part of the experimentation, small samples were produced so as to increase the homogeneity of the samples; moreover the samples were directly cast in the mould to separate the effect of the pressure from the effect of the cooling rate. The second step of the study was to cast larger samples to evaluate the effect of the size on the casting properties. A laboratory squeeze casting machine was constructed on purpose to produce cylindrical aluminium alloy ingots at different squeezing pressure and mould temperature.

Two different sets of samples were produced by using the same machine but different dies; the process parameters are reported in Table 4. For both sets, the squeezing pressure was applied for 30 s and it ranged from 0 to 100 MPa. Actually, also for 0 MPa, a minimum pressure was applied to enhance the ingot solidification. The first set of samples (100 mm in length and 30 mm in radius) was produced to evaluate the effect of the squeezing pressure on the distribution of the mechanical properties. In the second set (120 mm in length and 48 mm in diameter) the mould temperature was also changed to investigate the combined effect with the pressure. Two nominal mould temperatures were used even if small deviations were measured during the experimental practice.

First set of samples					
Sample	*Applied pressure [MPa]*	*Melt temperature [°C]*	*Mould temperature [°C]*	*Delay time [s]*	*Pressure time [s]*
A	0	750	350	15	30
B	50				
C	75				
D	100				
Second set of samples					
Sample	*Applied pressure [MPa]*	*Melt temperature [°C]*	*Mould temperature [°C]*	*Delay time [s]*	*Pressure time [s]*
a	0	750	300	10	30
b	50				
c	75				
d	100				
e	0	750	350	10	30
f	50				
g	75				
h	100				

Table 4. Process parameters for the two set of samples.

In the final equipment, the lower die was designed without any mould separation (useful for the sample extraction) to avoid flash during squeezing: Figure 12 reports the squeeze casting apparatus and some cast ingots. The pressure was applied by means of the upper plug whereas the lower mould was fixed to a support that was fixed in turn on a basement. A pin was inserted in the plug to allow the ingot extraction at the end of the cooling stage. The mould presented a hole for the insertion of a K-type thermocouple. An hydraulic cylinder was used to provide the pressure on the plug that was fixed to it. A hollow thermostatic oven was used to keep in temperature the mould.

At each casting operation, a portion was cut from the as-received ingot, afterwards it was put into a graphite crucible and molten in a muffle. When the melt temperature reached a temperature about 750 °C, it was poured in the mould. The mould was preheated by means of the hollow oven. About 2 s were necessary to pour the melt into the mould and other 10-15 s elapsed before the application of the squeeze pressure (due to the time for the plug

approach). After the squeezing, the hollow oven was removed and the mould was left to cool in air. During the first stages of the ingot casting, the mould temperature was acquired.

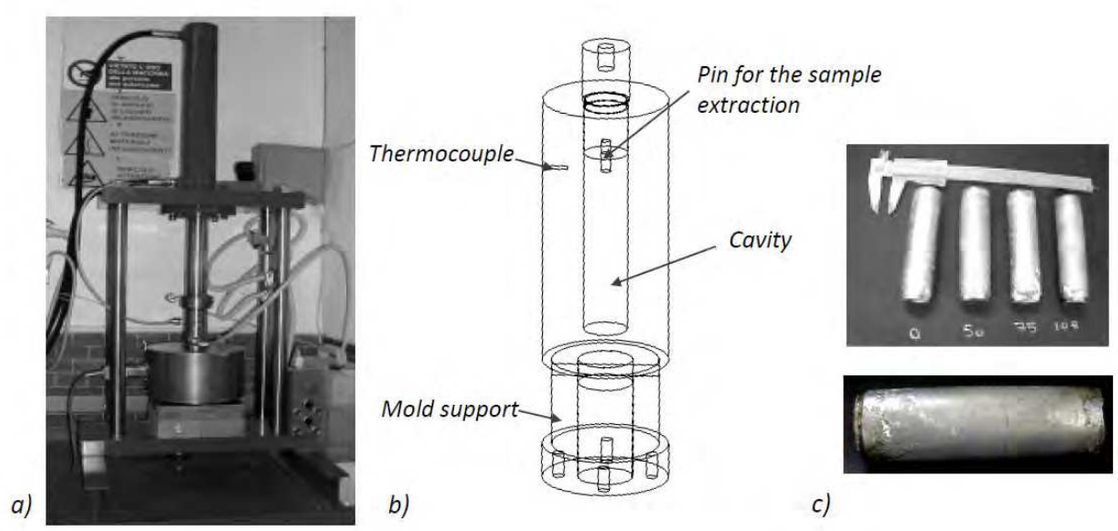

Fig. 12. (a) The experimental apparatus; (b) a sketch of the mould for the direct squeeze casting; (c) cast ingots.

At the end of the cooling, each cast ingot was extracted only by moving the plug thanks to the pin inserted into the plug (Figure 12). In order to evaluate the effect of the squeezing pressure on the ingot surface properties, the roughness of each ingot was measured along the cylinder height. Four measurements were performed at 90° of angular spacing. In analogy with the experimentation on the small samples, each ingot was cut and each section was preliminarily subjected to metallographic preparation and etched to reveal the microstructure. FIMEC and Vickers microhardness tests were performed as well. In particular, the microhardness was measured along the radius of the sections as well as the alloy dendrite size. Instead, the FIMEC test was performed only at the centre of the sections.

5.2 Experimental results

5.2.1 Effect of the squeezing phase on the mechanical property distribution

The effect of the squeezing phase on the casting properties is evident in all the ingot characteristics (Table 5). The surface aspect is clearly dependent on the pressure due to the better metal-mould matching during squeezing. Roughness is strongly dependent on pressure not only in terms of mean value over the surface but also for dispersion. Moreover, the comparison between the different microstructures, for the maximum and minimum applied pressure, in two different positions (the centre and the edge) underlines that the microstructure is strongly affected by the pressure (Figure 13). Also in these ingots, the microstructures show primary aluminium dendrites, particles and eutectic constituents but a different dendrite size distribution is observed across the sample. The dendrite size appears to be comparable for all the pressures near the sample skin.

	FIMEC Test	**Roughness (Ra)**			**Micrographs**	**Microhardness**
Sample	*Yielding stress in the centre*	*Mean value*	*Dispersion*	*Distance from the centre*	*Dendrite cell size*	*Vickers microhardness*
	[MPa]	*[µm]*	*[µm]*	*[mm]*	*[µm]*	*[HV]*
A	120.4	3.08	0.82	1	50.1	80.2
				6.5	35.7	95.2
				8	31.3	98.1
				13	18	103.4
B	130.5	0.32	0.13	1	35.7	82.7
				6	27.5	91.4
				13	15.9	103
C	144.0	0.36	0.07	1	28.6	84.8
				6	25.8	95.6
				13	16.3	111.6
D	204.5	0.39	0.05	1	29.6	94
				7	27.1	103
				13	17.6	103.4

Table 5. Mechanical, microstructural and morphological data extracted from squeezed samples in different points.

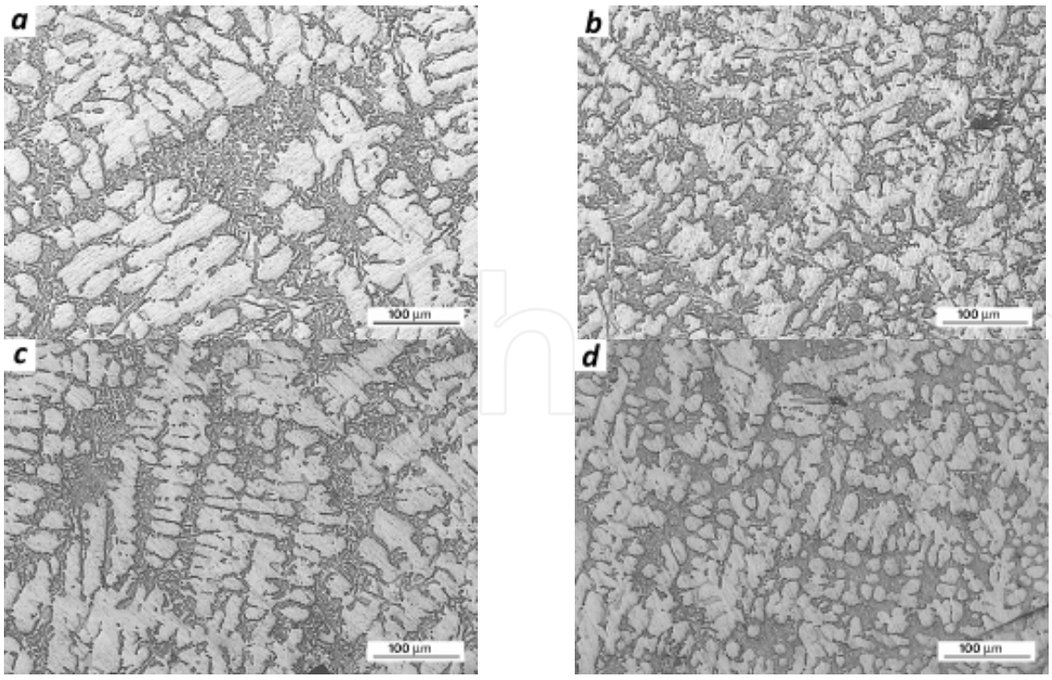

Fig. 13. Micrographs of metallographic sections: sample A (solidified without squeezing) in the middle zone (a), and in the edge (b); sample B (at the squeezing pressure of 100 MPa) in the middle zone (c), and in the edge (d).

Figure 14 shows the experimental curves obtained from microhardness tests (Figure 14-a) and FIMEC tests (Figure 14-b). The higher the pressure, the higher the microhardness: also data scattering reduces due to the squeezing. The pressure has a significant effect on the entire FIMEC curve as it shifts toward higher force values, by increasing pressure.

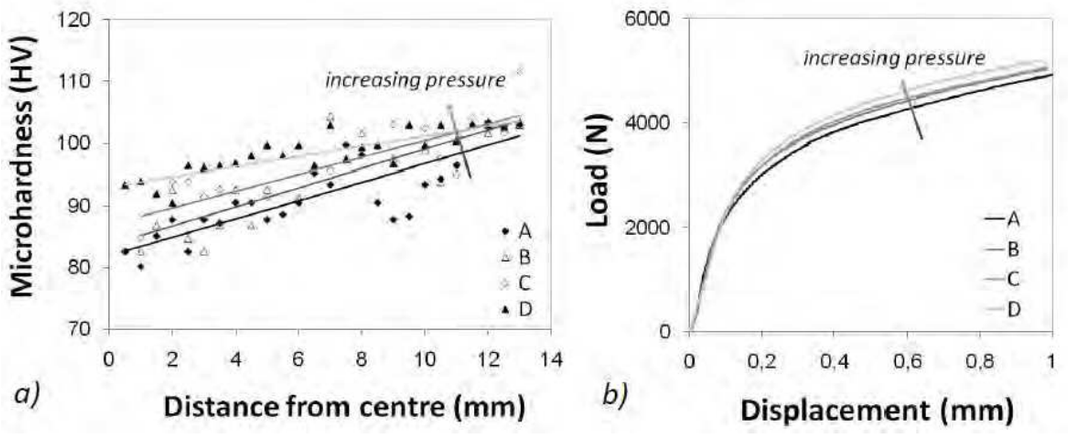

Fig. 14. Mechanical tests for all the squeezing pressures: (a) microhardness profiles along the sample radius; (b) FIMEC tests at the centre.

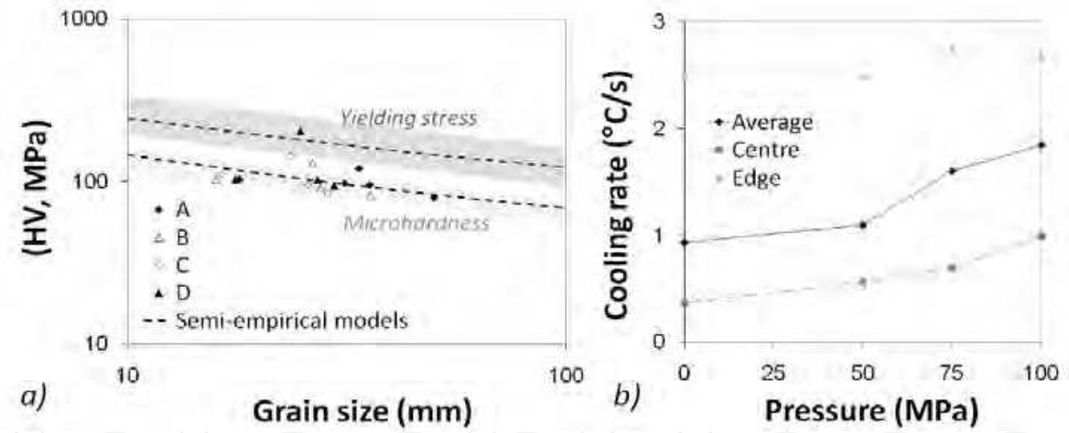

Fig. 15. Theoretical predictions: (a) comparison between experimental and predicted data for mechanical properties; (b) cooling rate inference by microhardness values at different squeezing pressures.

Microhardness is directly correlated to the microstructure. A similar value is measured near the skin for all the squeezing pressures whereas a significant difference is observed toward the centre. Moreover, a higher data scattering is observed at lower pressure values. At 100 MPa, the trend tends to be an horizontal line and a lower dispersion is measured. Microhardness and dendrite size values of Table 5 are evaluated in the same points along the radius. Instead the yielding stress is always evaluated at the centre of the samples. Experimental values for yielding stress and microhardness are reported in Figure 15-a together with the theoretical trends extracted respectively from equation (1) and (2). The semi-empirical models were fitted by using the constants described in the previous section and obtained by squeezing tests on small samples of the same alloy. There is a good agreement

between experimental data and predicted ones. A worse agreement is observable for the yielding stress and is probably due to the higher size of the zone interested to the indentation.

As experimental data are in agreement with predictions of equation (1) and (2), it is expected that equation (4) and (5) can be used for the same alloy to infer cooling rate during solidification. In Figure 3-b, microhardness values of Table 5 were used to infer cooling rate at the different squeezing conditions in three sample positions. It is evident that the cooling rate is similar near the edge for all the squeezing pressures.

Cooling rate can be extracted from cast parts by means of a simple indentation test. This is an important operation not only to provide correct inputs for numerical simulations, but above all, to optimize the casting process itself. In fact, it is difficult to define a precise correlation between process parameters and cycle time. Moreover, the cycle time is strongly dependent on the cooling rate. In die casting optimization, performing simple indentation tests on the first cast parts could allow to rapidly converge towards the process optimum. Material equations (4) and (5) were fitted once starting from laboratory specimens but they are applicable on cast products for every casting condition. It is hence possible to characterize all the alloys of interest and use the results to calibrate industrial processes.

5.2.2 Combined effect of the squeezing pressure and the mould temperature

The thermal behaviour of the ingot and the mould in direct squeeze casting is very complex. Sometimes, the experimental evidence could be quite different from the expected trends. In Figure 16, the cast ingots are shown for the nominal mould temperature of 300 °C: the surface appearance is put in evidence together with the typical microstructure. The average roughness for the same ingots is reported in Figure 17. The roughness is expressed in terms of mean value and dispersion for each sample.

In Figure 18, all the results from the mechanical characterization are shown. From the flat indentation tests, the load at the displacement of 0.4 mm was acquired and reported in Figure 18-a in terms of mean value and dispersion for each ingot. Figure 18-b shows the microhardness profile along the cylinder axis for two samples cast at different mould temperature and squeezing pressure. The profile is qualitatively similar with a minimum in the centre. The microhardness mean values and dispersions are reported in Figure 18-c. The hardness increase is strictly dependent on the microstructure refinement (Figure 16).

In the reported experimentation, fixing the mould temperature and the squeezing pressure, the highest ingot cooling rate would be expected for the lower mould temperature as in the initial stage the ingot is cooled by the heat transfer with the steel mould. The mould heating rate should be the lowest as well. But experimental measurements show that the highest mould heating temperature is related to the mould temperature of 350 °C instead of 300 °C. That is due to the transient phase between the beginning of the melt pouring and the pressure application. In those 12 s, the molten metal can suddenly solidify, affecting the heat transfer during the squeezing. As a consequence, best mechanical properties are obtained at the higher mould temperature at which the melt solidification mainly occur during squeezing. This is evident both from FIMEC data (Figure 18-a) and microhardness data (Figure 18-b). At the same mould temperature, mechanical performances generally increase with applied pressure. Data scattering is high due to several occurrences during casting; such as the formation of an oxide coating on the air exposed melt surface or the turbulence of the molten metal during pouring.

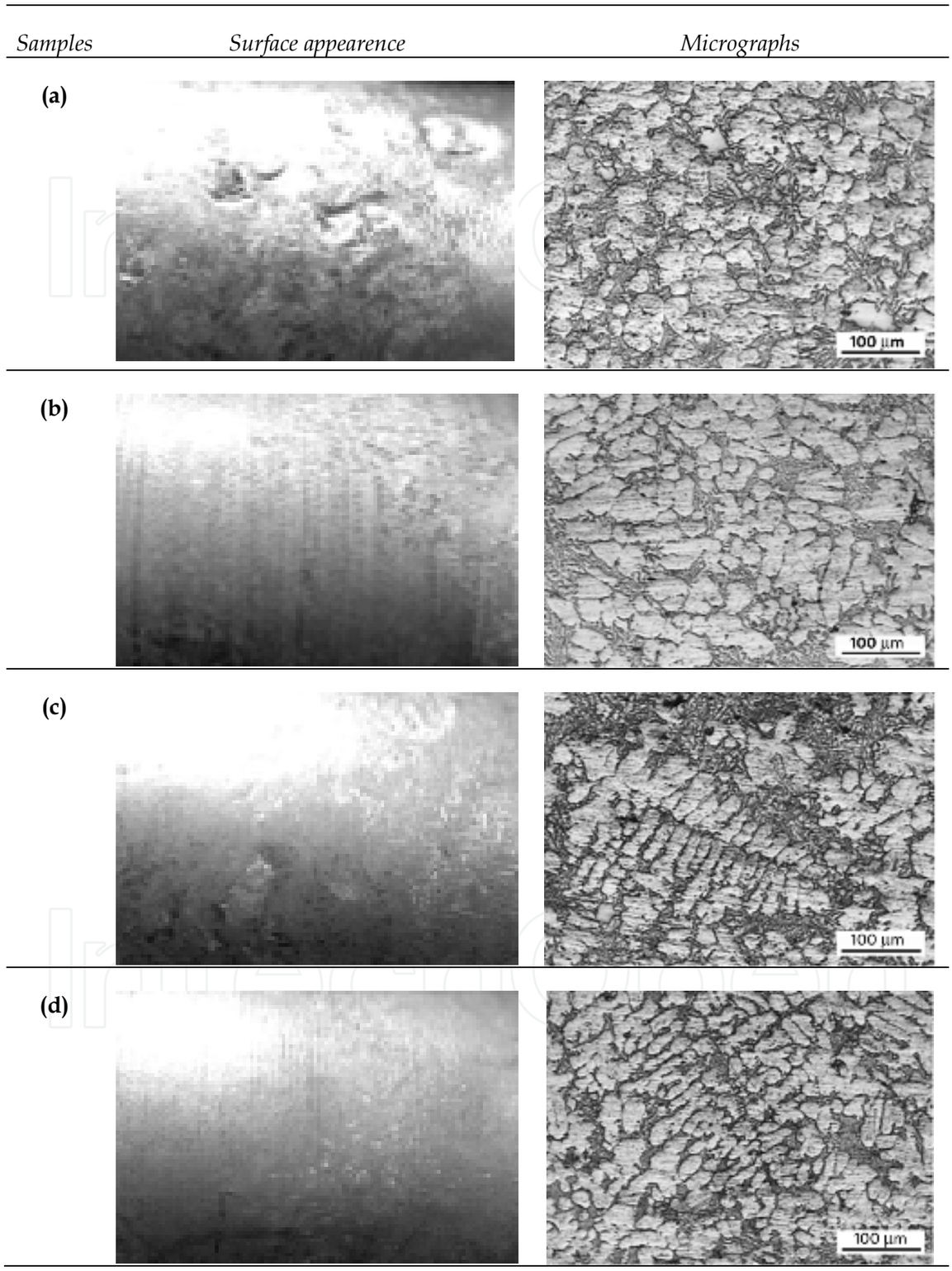

Fig. 16. Surface appearance and micrographs of the ingots produced at the lower mould temperature: samples a, b, c and d.

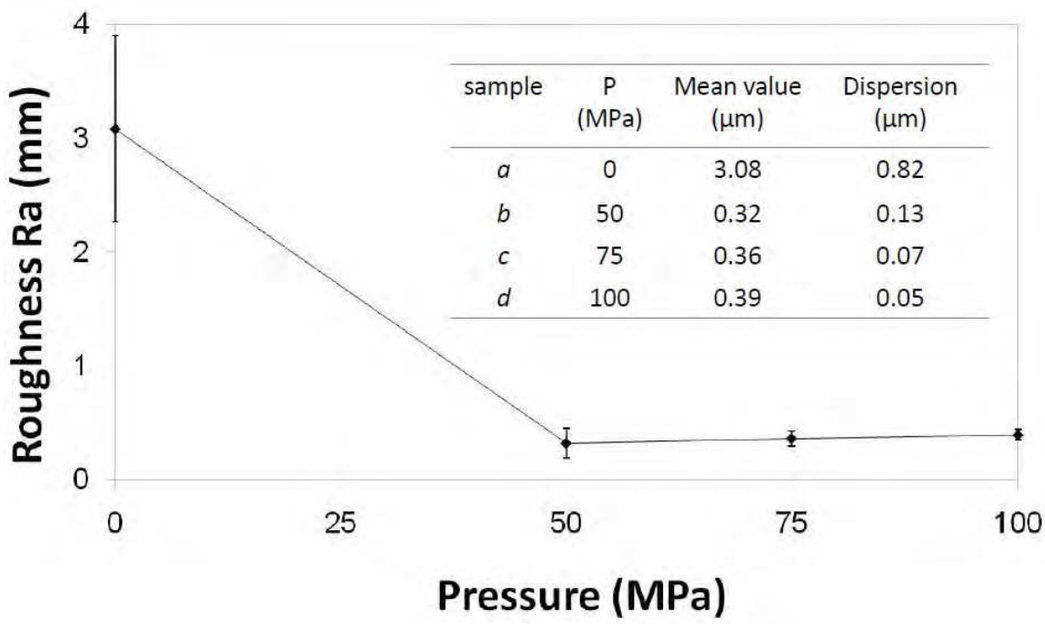

sample	P (MPa)	Mean value (μm)	Dispersion (μm)
a	0	3.08	0.82
b	50	0.32	0.13
c	75	0.36	0.07
d	100	0.39	0.05

Fig. 17. roughness for the ingots produced at the lower mould temperature: samples a, b, c and d.

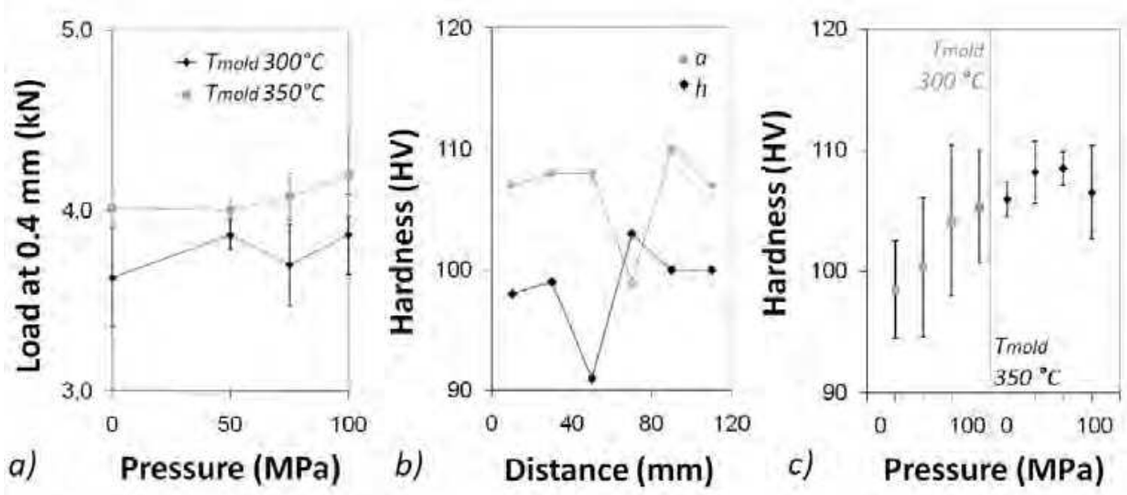

Fig. 18. Experimental results: mean indentation load (a), hardness profile along the cylinder height for the ingots *a* and *h* (b), mean hardness for all the ingots (c).

Figure 19-a reports the experimental heating curves of the mould in the first 80 s from the melt pouring: it is evident that higher temperature profiles are reached with lower squeezing pressures; some acquisitions were interrupted before 80 s for the occurrence of technical problems. However, the dependence of the mechanical performances on the final ingot cooling rate is always clear. From the value at 0 s, reported in Figure 19-a, it is possible to measure the real initial mould temperature. In the range between 40 and 80 °C the mould heating rate was extracted and related in Figure 19-b to the mean microhardness of the final ingot.

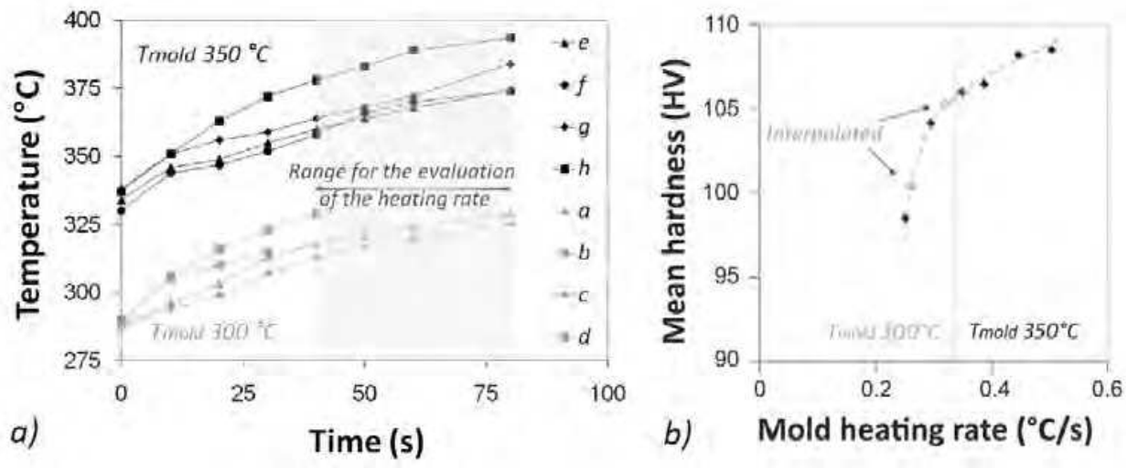

Fig. 19. Experimental results: heating curves of the mould during casting for all the ingots (a), correlation between the mould heating rate and the mean hardness (b).

The increase in the mould heating rate depends on the increase of the ingot cooling rate and therefore is related to the increase in the microhardness. The trend is evident and two points were interpolated to extract the mould heating rate for the castings that gave problems during the temperature acquisition. Higher mould heating rates (i.e. higher ingot cooling rates) lead to higher mechanical properties (Figure 19-b) because of the microstructure refinement (Figure 16). Moreover, the surface properties enhance due to the squeeze as Figures 16 and 17 show in terms of surface appearance and roughness.

5.3 Numerical simulation for the prediction of the ingot mechanical properties

Also in this case, a FE thermal model was defined to investigate the material behaviour during squeezing and to predict mechanical performances of the ingots. The model was calibrated by means of the experimental tests performed in the second set of samples. The FE model geometry was built according to the geometry of Figure 20-a, with a cavity of 28 mm radius and a length of 120 mm. A parametric approach was used by means of a batch procedure to easily modify geometrical and material parameters during the simulations.

In Figure 20-b the FE model is described. A 2D axisymmetric model was used, therefore the hole of the thermocouple was not modelled. The nodes at the interface between the mould and the plug were merged whereas an interface was modelled between the aluminium ingot and the steel mould. The interface was a thin (1 mm) layer which was put from the side of the mould and merged both to the ingot and to the mould. As initial condition, the aluminium ingot temperature was fixed to 750 °C whereas the mould temperature was put equal to the experimental mould temperature (i.e. 290 and 334 °C instead of the nominal values of 300 and 350 °C). A convection load was applied only to the lateral walls and typical values for convection in air were used (the bulk temperature T_b equal to the room temperature and the convection coefficient h equal to 10 W/m^2 K).

For the steel, general material properties of an AISI steel were used as well as general properties of an aluminium alloy were considered. Only the solidus and liquidus

temperature of the aluminium alloy were experimentally measured as they significantly affect the beginning and the end of the solidification. Figure 21 shows the heating and cooling curve of an aluminium alloy sample; this curve was obtained by immerging the thermocouple into the melt. Considering a fusion heat of 390 J/g, a specific heat of 0.88 J/g °C and the acquired solidus and liquidus temperatures, the enthalpy curve of Figure 20-b was constructed.

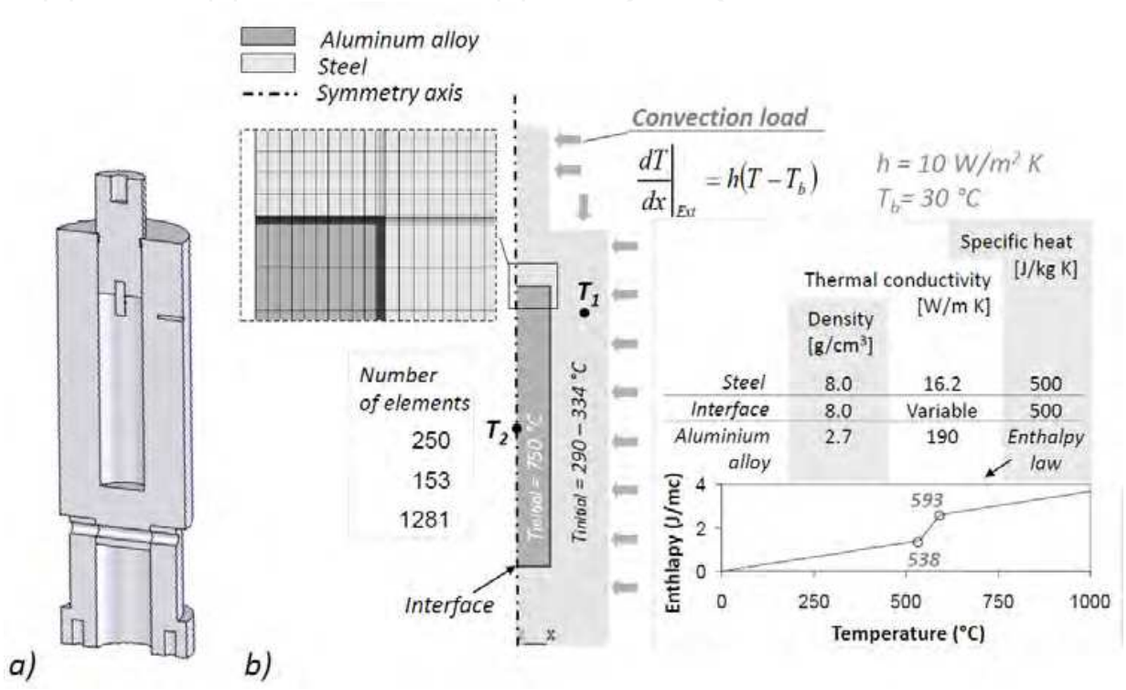

Fig. 20. Numerical modelling: (a) section of the squeezing system; (b) 2D mesh, loads and material properties used in the simulation.

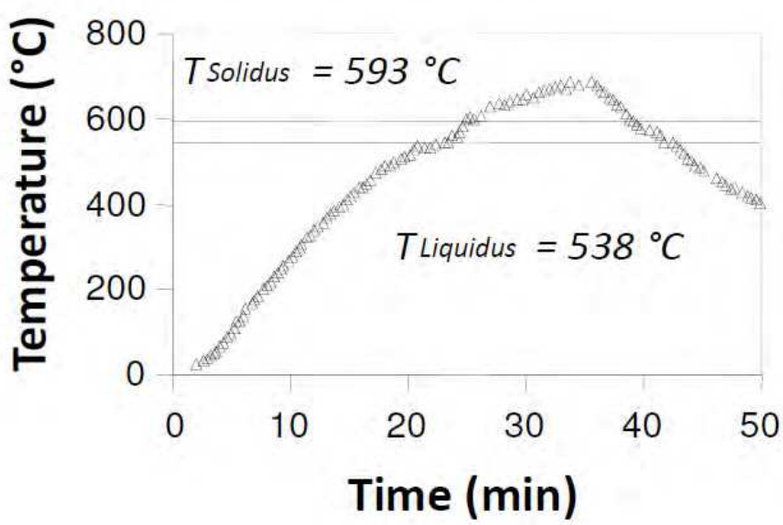

Fig. 21. The heating-cooling curve for the aluminum alloy.

The interface material had the same properties of the steel of the mould except for the thermal conductivity. This datum was used to take into account the different squeezing pressures. As squeezing determines a better matching between the aluminium ingot surface and the mould, this effect can be modelled by increasing the thermal conductivity of the interface material. This assumption allows to simplify the model and to reduce the time for the simulations.

In Figure 20-b there are reported two reference nodes for the temperature acquisition. The first point T_1 represents the thermocouple position in the experimentation. The point T_2 is at the centre of the ingot to evaluate to thermal history of the aluminium alloy during the solidification.

In Figure 22 typical results of the FE model are shown in dependence of the nominal mould temperature and the interface thermal conductivity. The results are expressed in terms of temperature evolution during time for T_1 (Figure 22-a) and T_2 (Figure 22-b). During the ingot cooling, the mould temperature increases up to a maximum due to the heat provided by the ingot solidification (Figure 22-a). Subsequently the temperature decreases due to the convection load. By increasing the nominal mould temperature, the temperature curves are vertically shifted. By increasing the interface thermal conductivity, the temperature peak is shifted at lower times and higher values due to the faster ingot solidification. During the alloy solidification, the ingot temperature decreases following a three stage curve (Figure 22-b). The first stage has a high slope and is representative of the molten metal cooling. At the beginning of the solidification the curve slope decreases. It increases again only at the end of the solidification.

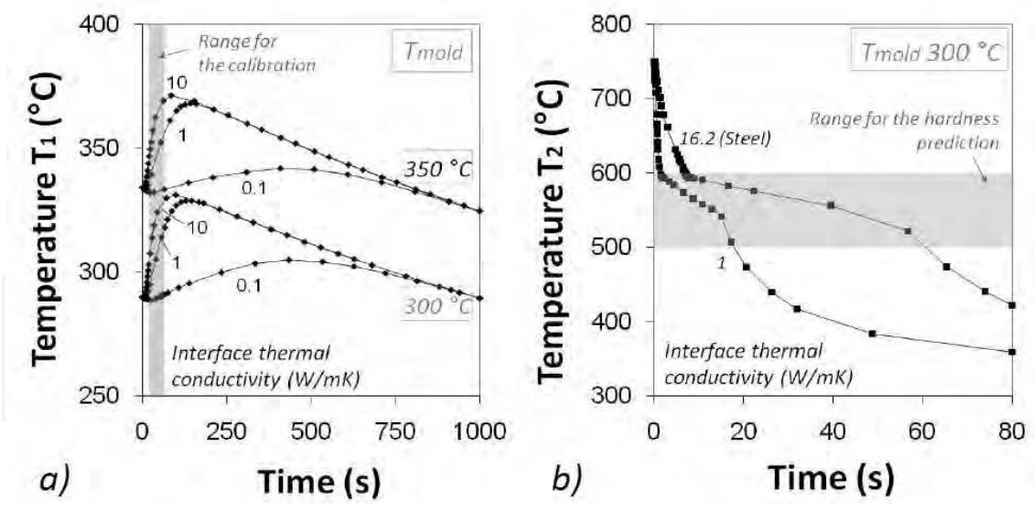

Fig. 22. Temperature evolution for T_1 (a) and T_2 (b) in different casting conditions.

The FE model was used to simulate the ingot cooling under different casting conditions. This goal was obtained by changing the mould temperature and the interface thermal conductivity. For each mould temperature (290 and 334 °C, nominally 300 and 350 °C), the thermal conductivity was changed from 0.1 to 25 W/m K. In order to extract a mould heating rate, the slope of the temperature curve at T_1 (Figure 22-a) was evaluated in the range between 50 and 90 s (as Figure 22-a shows). This numerical datum has to be compared

with the experimental datum of Figure 19-a for each casting (taking into account the delay time after pouring, about 10 s). Moreover, from Figure 16, the ingot cooling rate can be extracted for the same combination of mould temperature and interface thermal conductivity. The numerical ingot cooling rate was extracted in the range between 500 and 600 °C (i.e. around the alloy freezing range) as mainly in this temperature range the microstructure of the ingot is formed.

In order to predict the mechanical performances of the final ingots, the real thermal history of each ingot should be taken into account. Considering the experimental mould heating rate, it is possible to extract from Figure 23-a the thermal conductivity data that could provide the same heating rate with the model. Moreover, it is possible to extract from Figure 23-b the mould heating rate which is correspondent to the same thermal conductivity (and so to the same experimental mould heating rate). This way, any experimental occurrence that could affect the thermal behaviour of the ingot is compensated and the effective ingot cooling rate is obtained for each experimental acquisition of the mould heating rate. At the end, the numerical ingot cooling rates can be used in equation (1) to predict the ingot average hardness. In Figure 23-c the comparison between experimental hardness data and predicted data is shown for all the ingots. The figure underlines an optimal agreement between experimental and numerical data. This occurrence shows the suitability of equation (1) for the prediction of mechanical performances of aluminium alloy castings together with the validity of the proposed numerical procedure.

In conclusion it is possible to predict final mechanical properties of direct squeeze cast aluminium alloy parts. In this study, thanks to the simple ingot geometry, a 2D FE parametric model was used. After calibration, it is possible to use the model to infer from the measured mould heating rate, the numerical ingot cooling rate. This correlation has to be made only once and it is not necessary to run the solution for every change of the process parameters. Finally, the numerical ingot cooling rate is used to predict the ingot mechanical properties by using the proposed material equations (1) and (2) or other equivalent material laws.

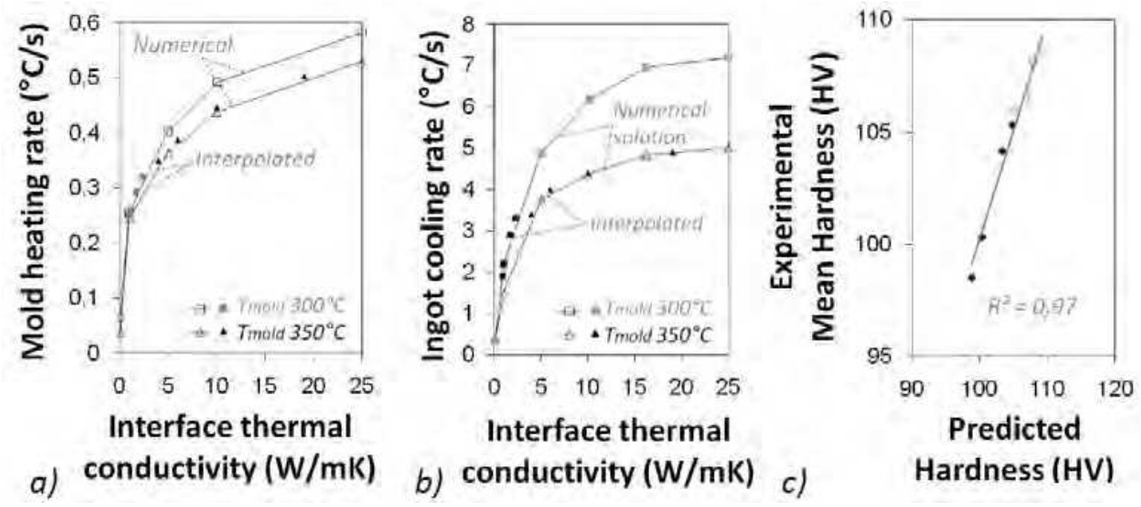

Fig. 23. Numerical results: mould heating rate (a) and ingot cooling rate (b) as a function of the interface thermal conductivity; comparison between experimental and numerical results (c).

Nomenclature

σ_Y	yield strength
σ_U	ultimate tensile strength
HV	Vickers hardness
σ_0, K_Y	constants of Hall-Petch equation for yield strength
HV_0, K_H	constants of Hall-Petch equation for hardness
λ	average dendrite cell size
ε	cooling rate
B, n	alloy specific constants in the relationship between λ and ε
C_Y, m	constants in the relationship between σ_Y and ε
C_H, m	constants in the relationship between HV and ε
q_Y, q_S	limit and saturation load values during FIMEC test
T	temperature
h, T_b	heat transfer coefficient and bulk temperature for convective load
R^2	correlation coefficient for linear interpolation

6. References

Britnell, D.J., Neailey, K. (2003) *Journal of Materials Processing Technology* 138 306-310.

Donato, A., Gondi, P., Montanari, R., Moreschi, L., Sili, A. and Storai S. (1998) "A remotely operated FIMEC apparatus for the mechanical characterization of neutron irradiated materials" *J.Nucl. Mater.* Vol. 258-263 pp. 446-451.

Gallerneault, M., Durrant, G. and Cantor, B. (1995) "Eutectic channelling in a squeeze cast Al-4.5wt%Cu alloy", *Scripta Metallurgica et Materialia,* Vol.32, No.10, pp.1553-1557.

Gallerneault, M., Durrant, G. and Cantor, B. (1996) "The squeeze casting of hypoeutectic binary Al-Cu", *Metallurgical and Materials Transactions A,* Vol.27A, pp.4121-4132.

Gondi, P., Montanari, R., Sili, A., (1996) "Small scale penetration tests with cylindrical indenters" *Proceedings of IEA international symposium Julich Germany*, pp.79-84.

Han, Y.S., Kim, D.H., Lee, H.I. and Kim, Y.G. (1994) "Effect of applied pressure during solidification on the microstructural refinement in an Al-Cu alloy", *Scripta Metallurgica et Materialia,* Vol.31, No.12, pp.1623-1628.

Hong, C.P., Shen, H.F. and Lee, S.M. (1998) "Prevention of macrodefects in squeeze casting of an Al-7 wt pct Si alloy", *Metallurgical and Materials Transactions B*, Vol.31B, pp.297-305.

Hong, C.P., Shen, H.F. and Cho, I.S. (1998) "Prevention of macrosegregation in squeeze casting of an Al-4.5 wt pct Cu alloy", *Metallurgical and Materials Transactions A*, Vol.29A, pp.339-349.

Kalpakjian, S. (2000), *Manufacturing processes for engineering materials – 3° Edition*, Addison-Wesley Publishing Company, ISBN 0-201-30411-2.

Kim, S.W., Durrant, G., Lee, J.H. and Cantor, B. (1999) "The effect of die geometry on the microstructure of in direct squeeze cast and gravity die cast 7050 (Al-6.2Zn-2.3Cu-2.3Mg) wrought Al alloy", *J. of Materials Science*, Vol.34, pp.1873-1883.

Lee, J.H., Won, C.W., Cho, S.S., Chun, B.S. and Kim, S.W. (2000) "Effects of melt flow and temperature on the macro and microstructure of scroll compressor in direct squeeze casting", *Materials Science and Engineering*, Vol.A281, pp.8-16.

Lee, J.H., Kim, H.S., Won, C.W., Cantor, B. (2002) *Materials Science & Engineering* A 338 182-190.

Maeng, D.Y., Lee, J.H., Won, C.W., Cho, S.S. and Chun, B.S. (2000) "The effects of processing parameters on the microstructure and mechanical properties of modified B390 alloy in direct squeeze casting", *J. of Materials Processing Technology*, Vol.105, pp.196-203.

Reed Hill, R.E. (1996) *Physical metallurgy principles*, third edition. PWS publishing Company, Boston. pp.192.

Savas, M.A., Erturan, H. and Altintas, S. (1997) "Effects of squeeze casting on the properties of Zn-Bi monotectic alloy", *Metallurgical and Materials Transactions A*, 1997, pp.1509-1515.

Shuangjie, C. and Renjie, W. (1999) "The structure and bending poperties of squeeze-cast composites of A356 aluminium alloy reinforced with alumina particles", *Composites Science and Technology*, Vol.59, pp.157-162.

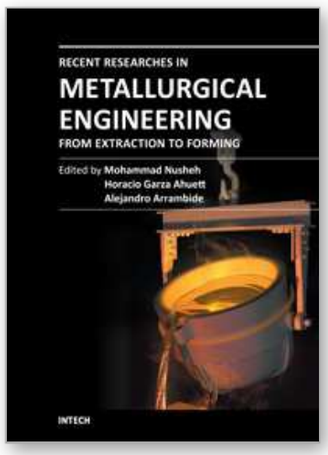

Recent Researches in Metallurgical Engineering - From Extraction to Forming

Edited by Dr Mohammad Nusheh

ISBN 978-953-51-0356-1
Hard cover, 186 pages
Publisher InTech
Published online 23, March, 2012
Published in print edition March, 2012

Metallurgical Engineering is the science and technology of producing, processing and giving proper shape to metals and alloys and other Engineering Materials having desired properties through economically viable process. Metallurgical Engineering has played a crucial role in the development of human civilization beginning with bronze-age some 3000 years ago when tools and weapons were mostly produced from the metals and alloys. This science has matured over millennia and still plays crucial role by supplying materials having suitable properties. As the title, "Recent Researches in Metallurgical Engineering, From Extraction to Forming" implies, this text blends new theories with practices covering a broad field that deals with all sorts of metal-related areas including mineral processing, extractive metallurgy, heat treatment and casting.

How to reference

In order to correctly reference this scholarly work, feel free to copy and paste the following:

Bellisario Denise, Boschetto Alberto, Costanza Girolamo, Tata Maria Elisa, Quadrini Fabrizio and Santo Loredana (2012). Squeeze Casting of Al-Si Alloys, Recent Researches in Metallurgical Engineering - From Extraction to Forming, Dr Mohammad Nusheh (Ed.), ISBN: 978-953-51-0356-1, InTech, Available from: http://www.intechopen.com/books/recent-researches-in-metallurgical-engineering-from-extraction-to-forming/squeeze-casting-of-al-si-alloys

INTECH
open science | open minds

InTech Europe
University Campus STeP Ri
Slavka Krautzeka 83/A
51000 Rijeka, Croatia
Phone: +385 (51) 770 447
Fax: +385 (51) 686 166
www.intechopen.com

InTech China
Unit 405, Office Block, Hotel Equatorial Shanghai
No.65, Yan An Road (West), Shanghai, 200040, China
中国上海市延安西路65号上海国际贵都大饭店办公楼405单元
Phone: +86-21-62489820
Fax: +86-21-62489821

IntechOpen